THE DESIGN AND SYNTHESIS OF FLUORESCENT DYES AS ENVIRONMENT-SENSITIVE MOLECULAR PROBES

by

Colin Wong

Submitted in partial fulfillment of the

requirements for Departmental Honors in

the Department of Chemistry and Biochemistry

Texas Christian University

Fort Worth, Texas

May 5, 2025

THE DESIGN AND SYNTHESIS OF FLUORESCENT DYES AS ENVIRONMENT-SENSITIVE MOLECULAR PROBES

Project Approved:

Supervising Professor: Sergei Dzyuba, Ph.D.

Department of Chemistry and Biochemistry

David Minter, Ph.D.

Department of Chemistry and Biochemistry

Keith Whitworth, Ph.D.

Department of Sociology and Anthropology

ABSTRACT

Fluorescent small molecule environment-sensitive probes have photophysical properties such as emission wavelength, fluorescence intensity or lifetime that change based on their surroundings like temperature, pH, or viscosity. Viscosity is an important physical property of fluid media, which plays crucial roles in many chemical and biological systems. In biological settings such as a cellular environment, changes in viscosity could be indicative of cellular malfunction or abnormalities. Thus, utilization of these environment-sensitive molecular probes could be useful in assessing the changes in viscosity of the cells. Ratiometric probes have two components with different reactive spectral properties that allow for more consistent internal calibration that provides more accurate determination of viscosity. However, the synthesis of ratiometric probes is often challenging, requiring multiple purification steps for isolation of the desired compounds. Therefore, this research highlights our synthetic efforts to make ratiometric molecular viscometers in a facile, efficient and modular manner.

INTRODUCTION

Viscosity is defined as the inverse parameter to fluidity and indicates a fluid's resistance to flow. This physical property plays an integral role in many biological and chemical contexts, especially those that are relevant to the complex microenvironments of living cells. Notably, viscosity of different regions of cells varies immensely, which affects the diffusion rates of various biological substrates in those respective areas. Importantly, abnormal changes in viscosity influence cellular processes such as signaling, material transport, and biochemical substance transfer processes (Ma et al., 2020). Key parts of the biological microenvironment that are affected by changes in viscosity are organelles such as lysosomes and mitochondria. Lysosomes are responsible for many processes related to aging and cellular damage, and viscosity plays crucial roles in keeping up with the correct enzymatic activity for degradation and molecular diffusion of waste products in the cell (Ma et al., 2020). Additionally, the mitochondria can be quite affected by changes in viscosity since many process such as cell metabolism, aging, autophagy, and tumorigenesis are viscosity dependent (Ma et al., 2020). Abnormal changes in mitochondrial viscosity can be signs of afflictions such as Parkinson's and Huntington's disease. This elicits the need to monitor viscosity of various cellular compartments as it serves as an indicator of potential life altering ailments (Ma et al., 2020).

The primary ways to measure viscosity of a fluid rely on large tools such as the falling ball viscometer, rotating viscometer, capillary viscometer and damping vibration viscometer. These methods effectively measure macroscopic, so-called bulk, viscosity; yet they are less suited for viscosity related to cellular type of environments (Ma et al., 2020). Thus, there has been an ever-growing interest in using small molecule probes as molecular viscometers. Such molecules, known as environment-sensitive probes (Klymchenko, 2017), could change their

photophysical properties in response to changes in the properties of the environment, including viscosity. From the synthetic standpoint, small molecule probes are very attractive as they allow for incorporation of various structurally and functionally diverse groups to tune the photophysical properties.

Fluorescence spectroscopy is a highly sensitive spectroscopic technique and a widely used tool for studying various biological processes (Kimball et al., 2015). This allows for visualization of these microscopic areas within a cellar compartment.

Various energy transfer mechanisms could be used for fluorescence-based viscosity measurements, including resonance energy transfer (RET), electronic energy transfer (EET), and fluorescence resonance energy transfer (FRET) (Fan et al., 2013). RET is the broad term that describes non-radiative transfer of energy from an excited donor to an acceptor. Both FRET and EET are subsections of this category. EET occurs through a longer distance, via dipole-dipole interactions, or closer range collisional transfer. FRET, when both molecules are fluorescent, transfers the excitation from one fluorophore (molecules that emit light upon excitation) to the other. FRET is the excited state transfer of a donor unit to an acceptor unit, within a distance of 1-10 nanometers (Figure 1) (Fan et al., 2013).

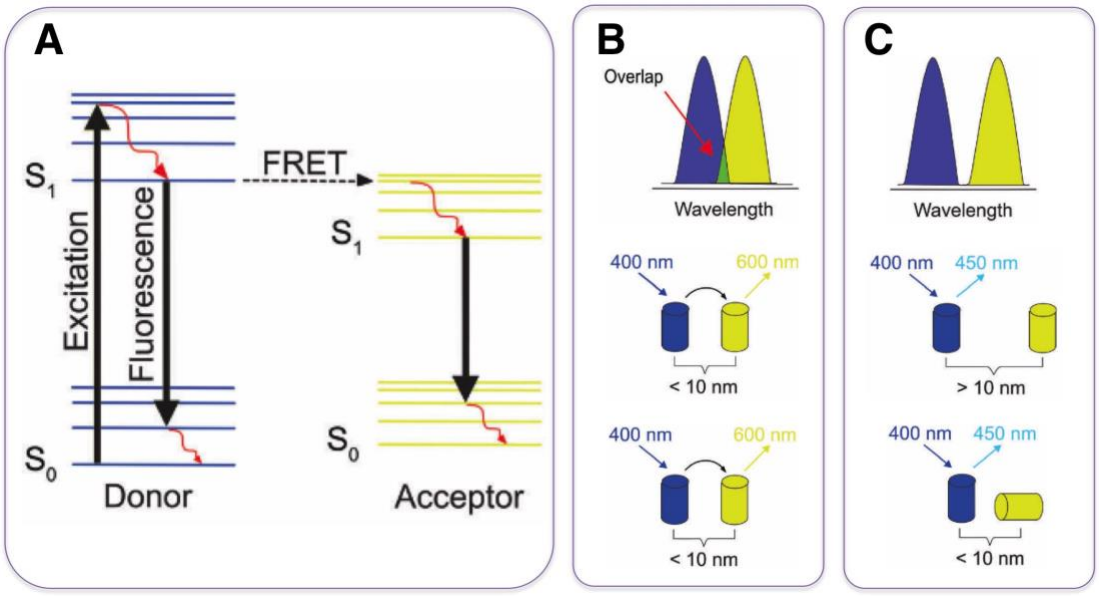

Figure 1. The process and requirements for FRET in donor and acceptor molecules. **A**: simplified Jablonski diagram for the energy levels and transitions associated with FRET; **B**: conditions for the donor (blue) and acceptor (yellow) moieties to allow FRET – spectral overlap (top), distance (middle), orientation (bottom); **C**: conditions for the donor (blue) and acceptor (yellow) moieties that prevent FRET – lack of spectral overlap (top), longer distance (middle), improper orientation (bottom) Adopted from: Teunissen et al., 2018.

Fluorescent molecules in which photophysical properties could be correlated with internal rotation within that molecule are known as molecular rotors. In general, a rotor refers to a scaffold to which an additional (auxiliary) group is attached, and this group rotates around the scaffold (Figure 2). The initial realization that these rotor-like molecules could report on the environmental viscosity variations was in 1980, when it was shown that the fluorescence intensity of some small molecules depends on the viscosity of the media (Paez-Perez & Kuimova, 2024).

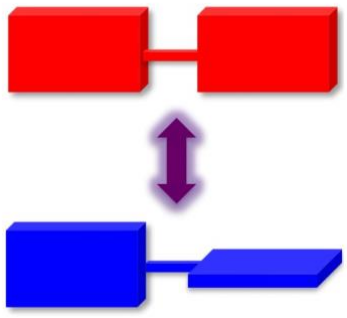

Figure 2. Concept of a molecular rotor. Rotation around the single bond of the two units leads to planar (red) and twisted (blue) conformers.

The molecular rotor has emerged as a key tool for measuring viscosity at the microscopic level since their fluorescence properties, specifically fluorescence intensity (Figure 3A), are directly influenced by molecular motion, making them particularly useful for tracking changes in viscosity. However, the polarity of various environments was seen to affect the excited state deactivation of some of these molecular viscometers, leading to skewed data that could not be decoupled from the viscosity determination. Furthermore, concentration of the fluorophores was shown to have a major effect on the observed fluorescence intensity. Especially in the heterogenous type of enviroments such as cellular compartments, the concentration of organic molecules could vary greatly, which in term will skew the viscosity measurements.

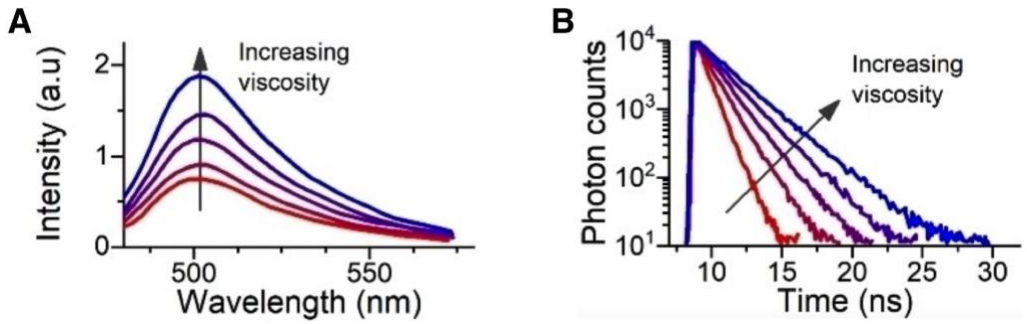

Figure 3. A: Intensity-based response of a molecular rotor to changes in viscosity; **B**: lifetime-based response of a molecular rotor to changes in viscosity (adopted from: Paez, et., 2024).

Additionally, other physical factors can affect the measurements of the environmentally sensitive molecular rotor such as pH, temperature, or an external substance concentration. Some fluorophores can be sensitive to both viscosity and pH, leading to an influenced response from the probe.

This led to the introduction of molecular viscometers those fluorescence lifetimes were used to track viscosity (Figure 3B). Compared to fluorescence intensity-based viscometers, the lifetime-based viscometers would be more immune to changes in the concentration of the fluorophore (Kuimova, 2012). However, lifetime-based molecular rotors might still give compromized measurments since organic molecules could aggregate in aqueous types of enviroments, and the lifetimes of the monomeric and aggregated states of the viscometer could be drastically different. In addition, the lifetime-based rotors could still undergo self-quench processes (similar to intensity-based probes).

Fluorescence Lifetime Imaging Microscopy (FLIM) allows the content to be spatially resolved, i.e., the data are taken across an image (Figure 4). This special resolution is done by using pulsed lasers that are able to detect a single photon or continuous wave lasers that modulate the phase of the photon (Kuimova, 2012). FLIM was useful for accessing viscosity of biological types of media, and it was shown to be independent of probe concentration, unaffected by optical setup artifacts, and bypasses medium transmissions properties. Unfortunately, FLIM requires unique, specialized instrumentation as well as expertise in data analysis and interpretation to accurately measure viscosity (Paez-Perez & Kuimova, 2024).

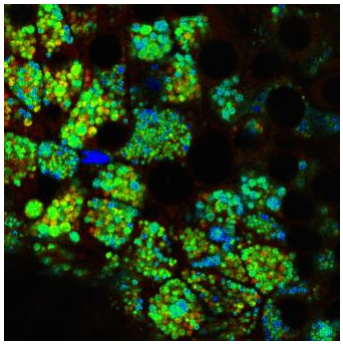

Figure 4. A typical FLIM of a cellular environment with a molecular viscometer (adopted from Requena et al., 2017).

Thus, ratiometric fluorescent probes have emerged as an alternative strategy to improve accuracy by reducing dependence on probe concentration and external environmental factors, while still allowing for operationally simple, inexpensive steady-state fluorescence measurements to be used for viscosity determinations. Fundamentally, a ratiometric viscometer is made up of two independent fluorophobic components (parts of the molecule that absorb and

emit light) (Kuimova, 2012). These ratiometric fluorescence probes are unique as they retrieve the intensity changes from two or more emission bands at different wavelengths, thus allowing for more accurate measurements (Gui et al., 2019). There are typically two types of ratiometric fluorescence probes: one that utilized an internal reference (fluorophore that is not sensitive to changes in viscosity), while the other type relies on conformationally flexible units, with their relative amounts (i.e., ratio) reporting on the changes of media's viscosity (Figure 5). The reference peak (Figure 5A) stays constant regardless of the different substances it is immersed in, while the intensity of the other peak increases due to increasing viscosity. To quantify these results, the ratio of intensity in the changing peak is divided by the intensity of the reference peak, allowing real-time and non-invasive measurements of viscosity to be retrieved (Paez-Perez & Kuimova, 2024). Similarly, for the conformer-based probe (Figure 5B), the ratio between two changing peaks is used to assess the viscosity of the media. In both cases, this internal normalization reduces errors from probe concentration, aggregation, or environmental impacts. Arguably, the two reversible signal changes are more sensitive than one-reference signal probes and offer better signal-to-noise responses in spectra measurements. In principle, the signals within the two reversible peaks are sensitive to energy transfers, charge transfers, proton transfers, chemical reactions, physical interactions, or binding events such as antigen-antibody or nucleic acid hybridization (Gui et al., 2019). Thus, the use of isomeric molecules with blocked internal rotations (i.e., non-rotors) is still needed to deconvolute other processes from the viscosity measurements.

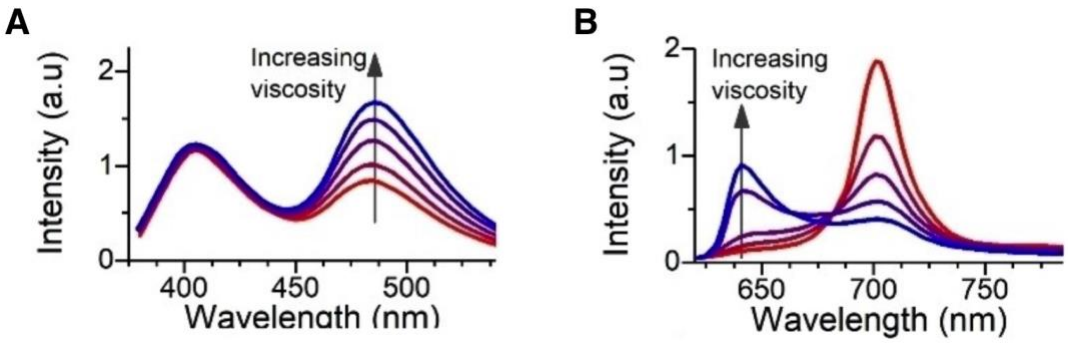

Figure 5. A: internal reference-based ratiometric rotor response to changes in viscosity (signal at ca. 400 nm is not changing as a function of viscosity, i.e., it is used as internal reference); **B**: conformer-based ratiometric rotor response to changes in viscosity (adopted from: Paez, et., 2024).

Synthetic accessibility (i.e., number of synthetic steps to make the molecules, availability of starting materials, ease of isolation and purification of the intermediates, etc.) as well as possibilities for tuning the photophysical properties of the probe are among the most important factors that one has to consider when designing a molecular viscometer. So called BODIPY, aza-BODIPY, and squaraine dyes are among most versatile fluorescent scaffolds (Figure 6). All these dyes have found numerous applications in various areas of chemistry, biology, and engineering (Das et al., 2023). Notably, these dyes are synthetically accessible in a facile, efficient and modular manner, and their photophysical characteristics (i.e., absorption and emission maxima in the visible and near-infrared regions of the electromagnetic spectrum (Das et al., 2023), lifetimes, etc.) can be tuned using a diverse range of reactions. Although, a number of rotors based on these scaffolds have been developed in the Dzyuba group (D. Ta, et al., 2024) over the last several years, ratiometric types of viscometers have not been reported.

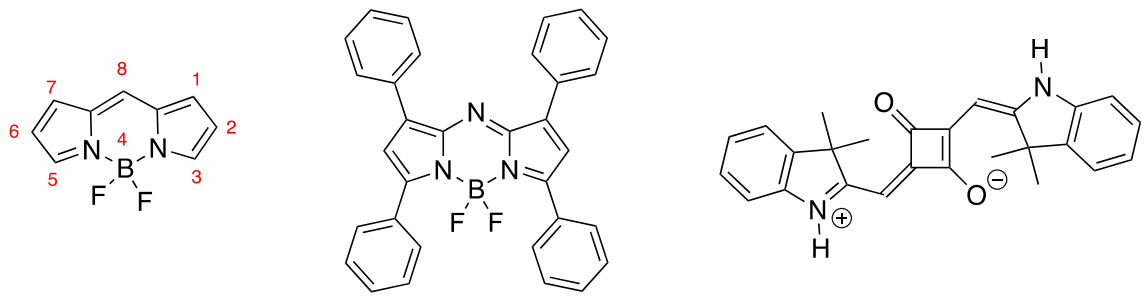

Figure 6. General structures of BODIPY (left), aza-BODIPY (middle) and squaraine (right) dyes. For BODIPY dyes, the positions on the BODIPY core are given by number; position 8 is also known as meso, positions 1 and 2 (as well as 6 and 7) are also known as α-position, position 3 (as well as 5) is also known as the β-position. Aza-BODIPY dyes follow the same numbering system as BODIPY dyes.

The focus of this research has been primarily developing BODIPY-based ratiometric viscometers. It is important to note that the BODIPY scaffold, unlike many other fluorescent scaffolds/dyes, offers the unique opportunity of generating both rotor-like and non-rotor examples using very similar or even identical synthetic approaches (Figure 7); thus, contributing further to the synthetic appeal of using this specific type of dyes. Specifically, the BODIPY rotor (**BODIPY R)** and BODIPY non-rotor (**BODIPY NR)** differ only by substituents in the 3- and 7-positions (see Figure 6 for specific numbering). H is smaller than a CH_3 group, which allows for the free rotation of the phenyl moiety around the BODIPY core; the larger CH_3-group restricts the rotation, which makes **BODIPY NR** a non-rotor. Notably **BODIPY R** and **BODIPY NR** are isomers of each other; thus, their solubility, responses to changes in media pH, polarity, and etc. should be very similar. Hence, any changes in the behavior of these two dyes would be related to

changes in ability to internally rotate. Thus, the use of two dyes should unambiguously indicate whether changes in photophysical properties are due to changes in viscosity associated with changes in other parameters.

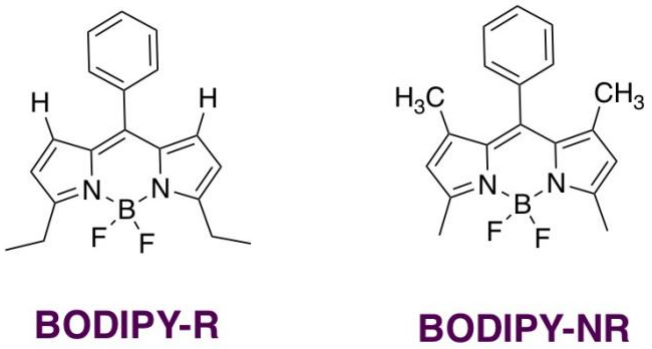

Figure 7. Representative structures of BODIPY-rotor (**BODIPY-R**) and BODIPY-non-rotor (**BODIPY-NR**).

From the fundamental perspective, excitation of the BODIPY dye (shown in red) should lead to the energy transfer to the aza-BODIPY part of the molecule (shown in blue) (Figure 8) if the transition moments of the two fluorophores (i.e., BODIPY and aza-BODIPY) are aligned; i.e., located in the same plane, which would be the case in low viscosity media. In practical terms, exciting the BODIPY unit with 480 nm light, leads to emission from the aza-BODIPY at 700 nm. Conversely, in high viscosity media, where the internal rotation is hindered, the energy transfer in the excited state would be inhibited; and excitation of the BODIPY units would only produce the emission from the same BODIPY units. In this case, the excitation of the BODIPY units with 480 nm light, led to emission of 525 nm light. It should be noted that the same arguments would be true for the BODIPY-aza-BODIPY system (i.e., dimeric, rather than

trimeric viscometer); however, from the synthetic standpoint synthesis of disubstituted aza-BODIPY scaffold appeared to be much more viable.

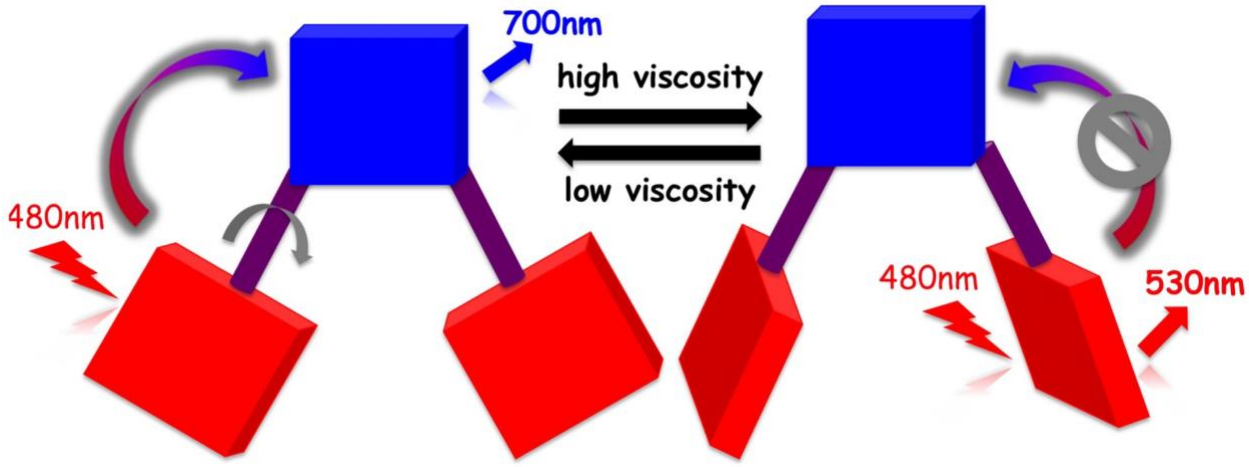

Figure 8. General representation of the ratiometric rotor and associated transfer process leading to respective emissions that could act as a viscometer. BODIPY units are shown in red, aza-BODIPY unit is shown in blue.

Previous research in the group focused on the conjugation of BODIPY and aza-BODIPY scaffolds using alkyne tethers in an effort to obtain ratiometric viscometers (Figure 9). The results confirmed the general hypothesis (Figure 8) for the viscometer designs. Specifically, in the case of rotor **1**, excitation of the BODIPY unit led to efficient transfer to the aza-BODIPY unit in low viscosity media (Figure 9A). Upon increasing the viscosity of the media (i.e., increasing the content of the more viscous component, glycerol), the emission from the aza-BODIPY unit decreased; and in glycerol, no transfer from BODIPY to aza-BODIPY was

obtained as evident by the emission from only the BODIPY unit. The non-rotor **2** was shown to be insensitive to the variation of the viscosity of the media (Figure 9B).

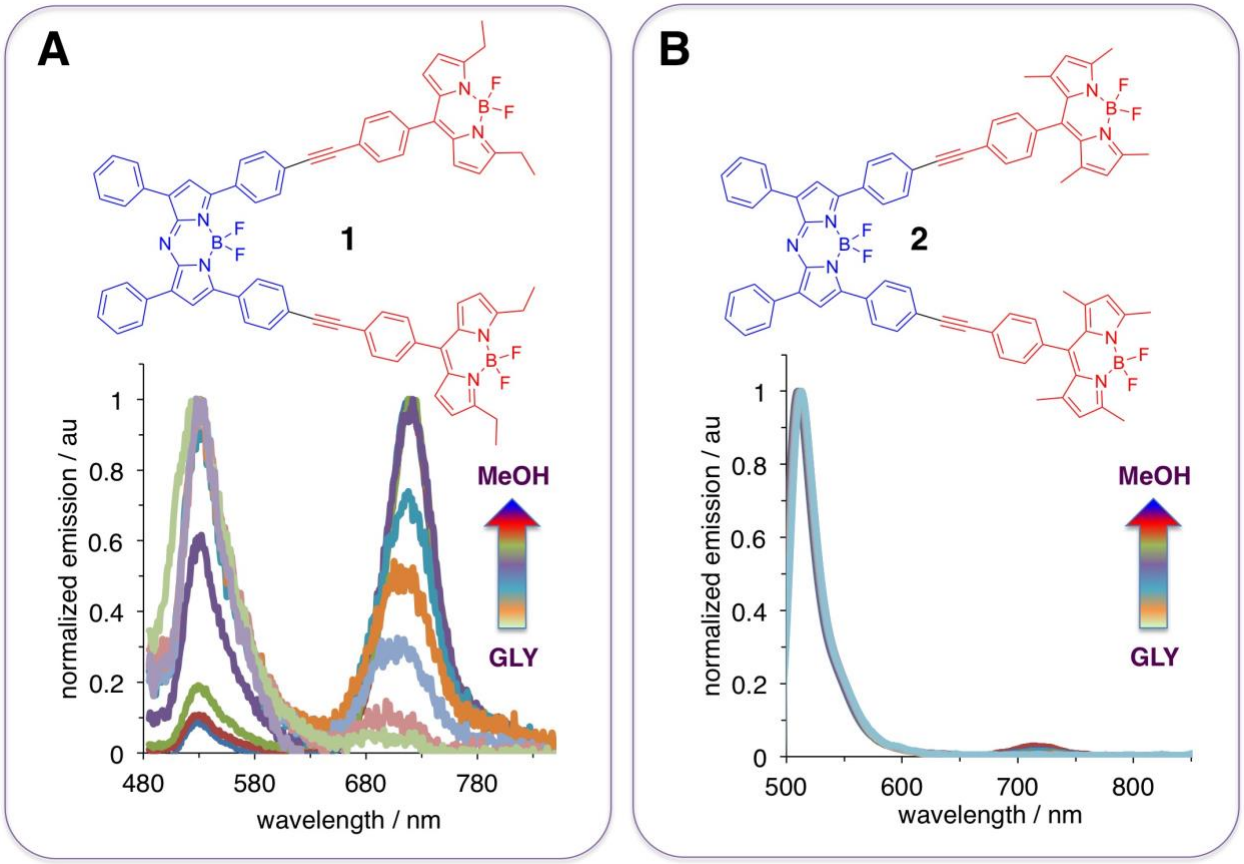

Figure 9. Structures of BODIPY-aza-BODIPY-BODIPY conjugates used as a molecular viscometer **1** (rotor) (**A**), and non-rotor **2** (control) (**B**) and their fluorescence responses to media of different viscosities (MeOH – low viscosity solvent, 0.7 cP; glycerol – high viscosity solvent, 1500 cP).

The aim of this research is to develop and optimize fluorescent small molecule environment-sensitive probes, using readily available and easily modifiable scaffolds, such as BODIPY and squarine dyes, which could respond to changes in viscosity in a ratiometric

manner. Thus, this work should contribute to the advancement of fluorescence-based sensing and imaging probes which is paramount for a range of applications such as medical diagnoses, cellular imaging, and biochemical analysis. (Liu et al., 2020);(Requena et al., 2017; Teunissen et al., 2018)

RESULTS AND DISCUSSION

Arguably, one of the main problems in the environment-sensitive probe development is to establish how structural characteristics of the probe could be related to the probe's performance. This largely stems from the fact that probes are discovered almost serendipitously, the synthesis is done in a non-modular manner, and in most instances use scaffolds that are not amenable to extensive pre/post-functionalizations. Therefore, one of the main goals for this research was to investigate how structural variations within a molecular viscometer could influence the viscosity measuring capabilities. A second objective was to develop more efficient synthetic procedures for assembling BODIPY-aza-BODIPY viscometers, considering some difficulties associated with the synthesis of viscometer **1** (Douady, et al., 2013-2015).

Since previous research demonstrated that conjugation of the BODIPY dyes to an aza-BODIPY scaffold produces a viable molecular viscometer (Figure 9), it was decided to synthesize molecular viscometer **3** (Figure 10), as a structurally related analogue of the viscometer **1**, which should address the first objective. The structural differences between viscometers **1** and **3** relate to the position of the rotating BODIPY units on the aza-BODIPY scaffold.

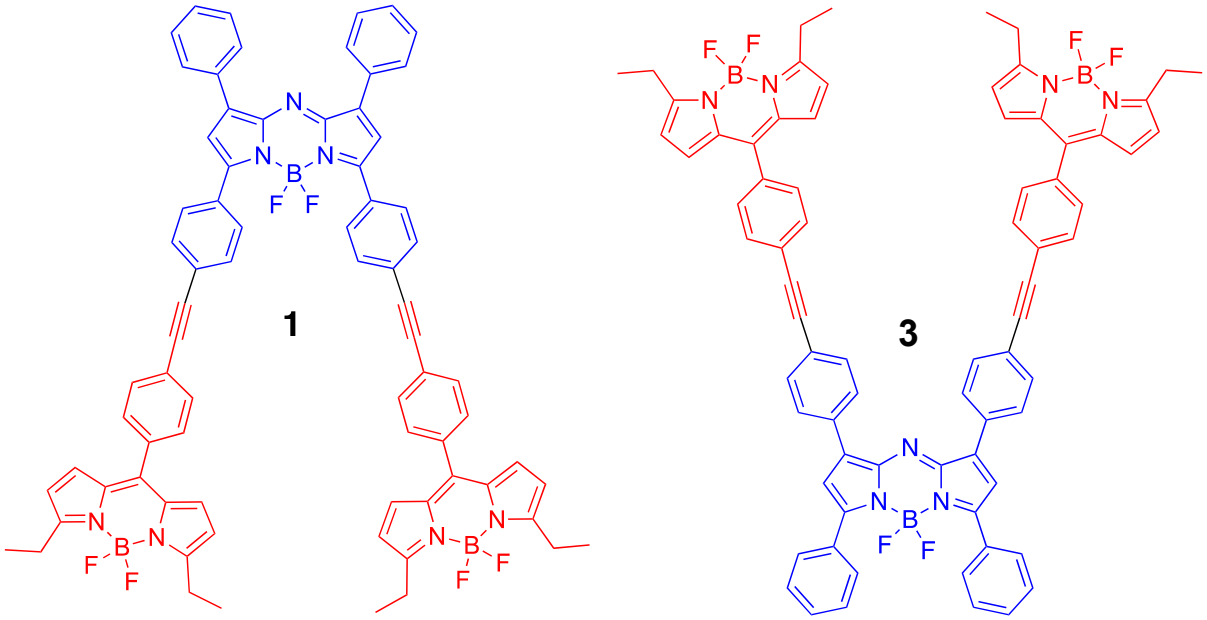

Figure 10. Structures of molecular viscometers **1** and **3**. BODIPY unit (red) and aza-BODIPY unit (blue).

The synthesis of dyes **1** and **3** relied on access to specifically iodo-substituted aza-BODIPY dyes **1.1** and **3.1**. Both of these aza-BODIPY dyes were prepared according to several well-established synthetic procedures (Scheme 1). Specifically, both syntheses started with an aldol condensation that involved an iodo-containing aldehyde or iodo-containing ketone, to give the respective enones **1.2** and **3.2**. The subsequent conjugate addition led to **1.3** and **3.3**, which were subsequently subjected to a cyclization reaction. These provided compounds **1.4** and **3.4**. Installation of the BF_2-functionality, using a literature procedure, gave the desired dyes **1.1** and **3.1** in ca. 15-20 % overall yields from commercially available starting materials.

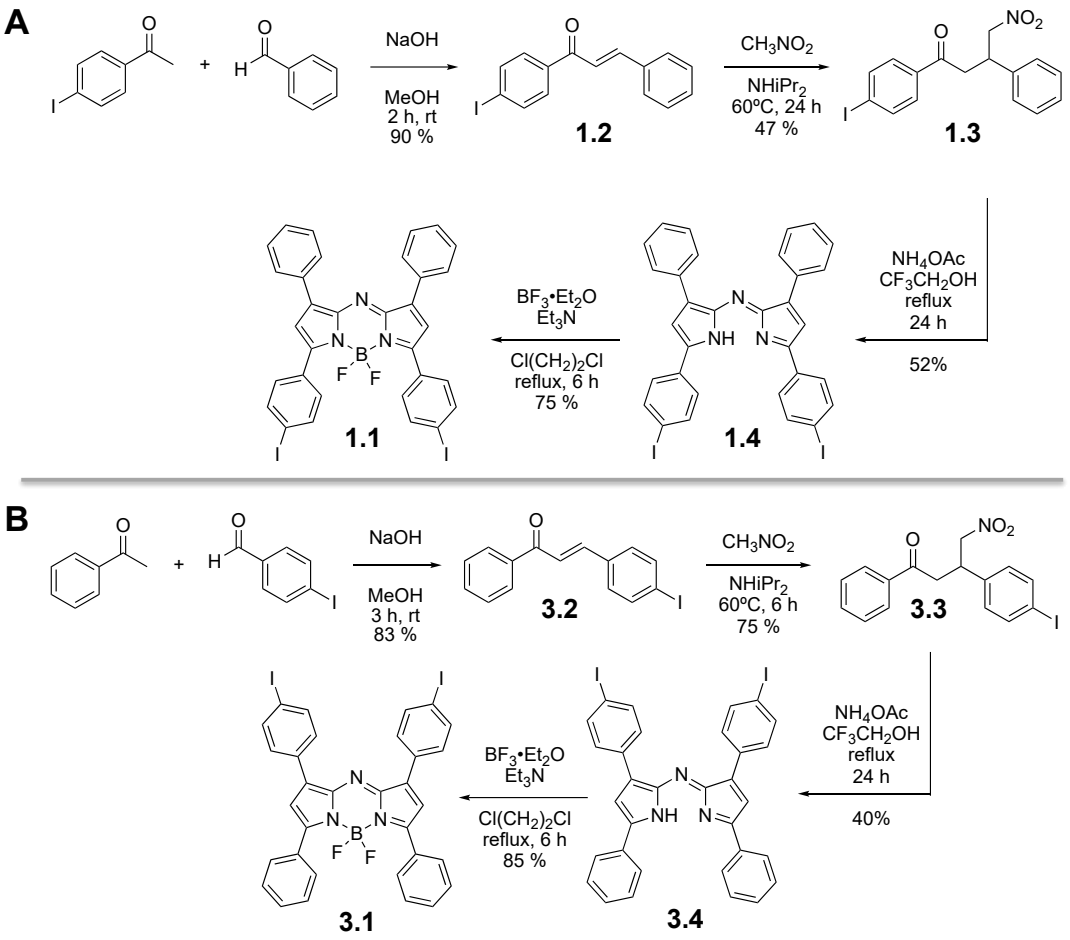

Scheme 1. Synthetic route to iodo-containing aza-BODIPY dyes **1.1** (A) and **3.1** (B).

BODIPY dye 4 was prepared using a solvent-free, mechanochemical approach (Scheme 2) according to the literature procedure (S.L. Raut et al., 2016).

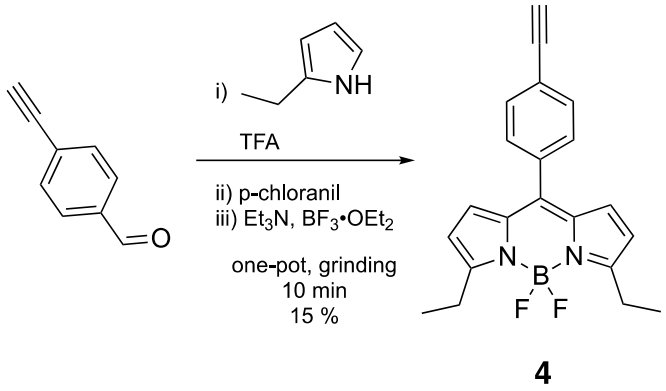

Scheme 2. Synthesis of BODIPY dye 4.

With BODIPY 4 and aza-BODIPY **1.1** and **3.1** in hand, the Sonogashira cross-coupling reaction was attempted (Scheme 3) (R. Chincilla et al., 2007). Regretfully, similar to previous experience (Douady et al., 2013-2015), the synthesis of **1.1** and **3.1** suffered from low yields under various conditions tested. Notably, even in the cases where the dyes were obtained, the reactions were found to be irreproducible at times. Furthermore, the purification process proved to be difficult and inefficient in providing dye **1**, for example, in sufficient purity required for spectroscopic studies. After a number of futile attempts to obtain dyes **1** and **3**, it was decided to revisit the structural requirements for the viscometer and attempt to explore other scaffolds.

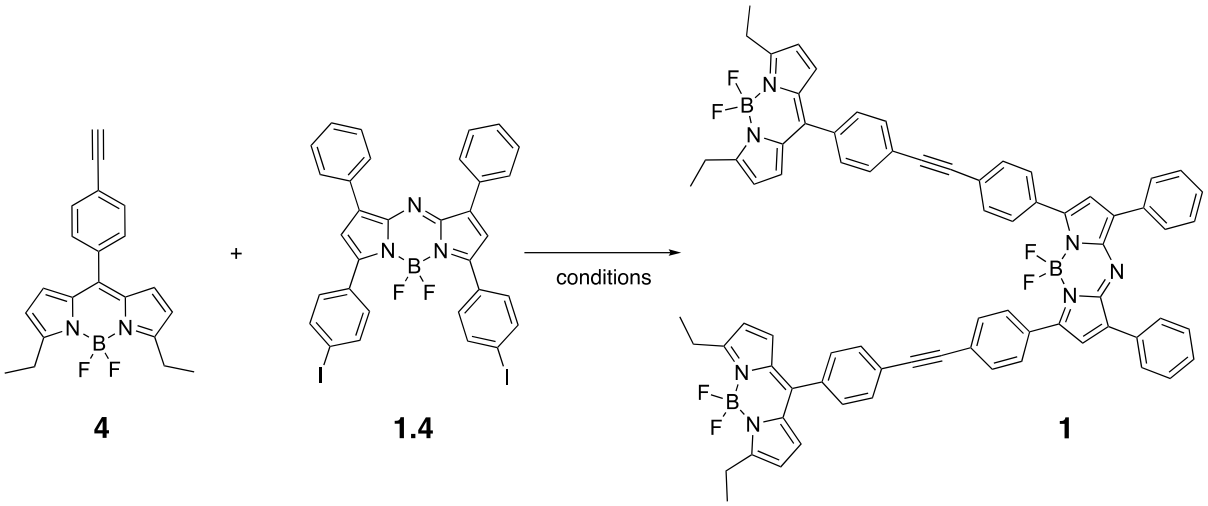

conditions	Yield / %
$Pd(PPh_3)_4Cl_2$, CuI, Et_3N, DMF, N_2, rt or Δ, 4 h – 12 h	0 – 5
$Pd(OAc)_2$, $NH_2(C_6H_4)CO_2H$, K_2CO_3, EtOH, rt or Δ, 12 h	0 – 5
$Pd(OAc)_2$, XPhos, Et_3N, rt, 12 h	3

Scheme 3. Attempted synthesis of dye **1** using the Sonogashira cross-coupling reaction.

Squaraine dyes (SQ) (Figure 11A) are another fluorescent small molecule scaffold that has been explored in the Dzyuba's laboratory in recent years (D. Ta et al., 2021);(D. Ta et al., 2023);(D. Ta et al., 2024). These dyes could be easily assembled via condensation of various nucleophiles with squaric acid (Figure 11B).

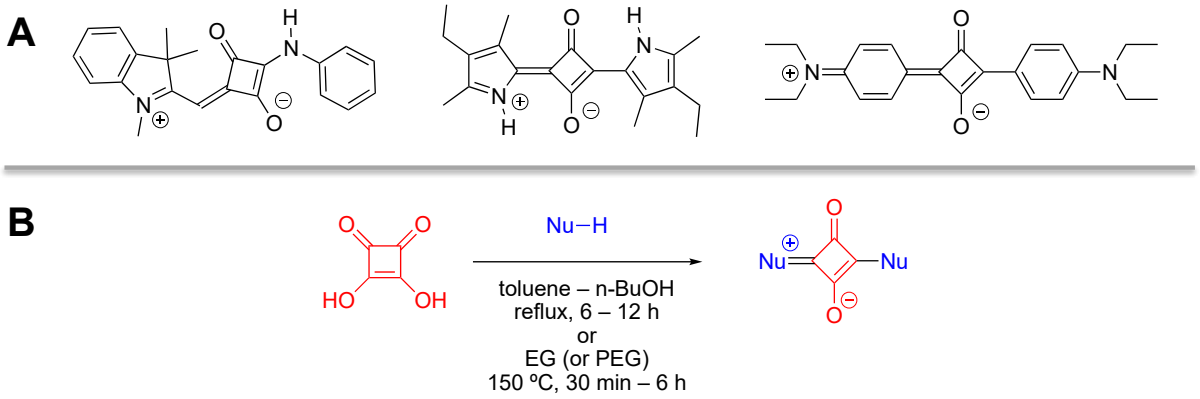

Figure 11. **A**: structures of several representative types of squaraine (SQ) dyes; **B**: general synthetic route to squaraine dyes from squaric acid (shown in red).

Considering the difficulties associated with metal-catalyzed cross-coupling reactions, it was decided to utilize metal-free, amide-bond formation for conjugation of the squaraine and BODIPY scaffolds to make **5** as the new type of molecular viscometer (Scheme 4).

Carboxylic acid-containing precursor **5.1** was readily available due to some unrelated studies conducted in the lab (J. M. Favret et al., unpublished results);(D. Ta et al., 2024). Using this lab procedure, squarine scaffold **5.2** was obtained in moderate yield. Availability of **5.2** also dictated the need for the synthesis of the amino-containing BODIPY dye **5.4** to achieve the subsequent formation of the amide bond. Dye **5.4** was obtained via a two-step process that relied on a mechanochemical synthesis of the nitro-containing **5.3**, followed by the reduction of the nitro functionality into the amine (Scheme 4).

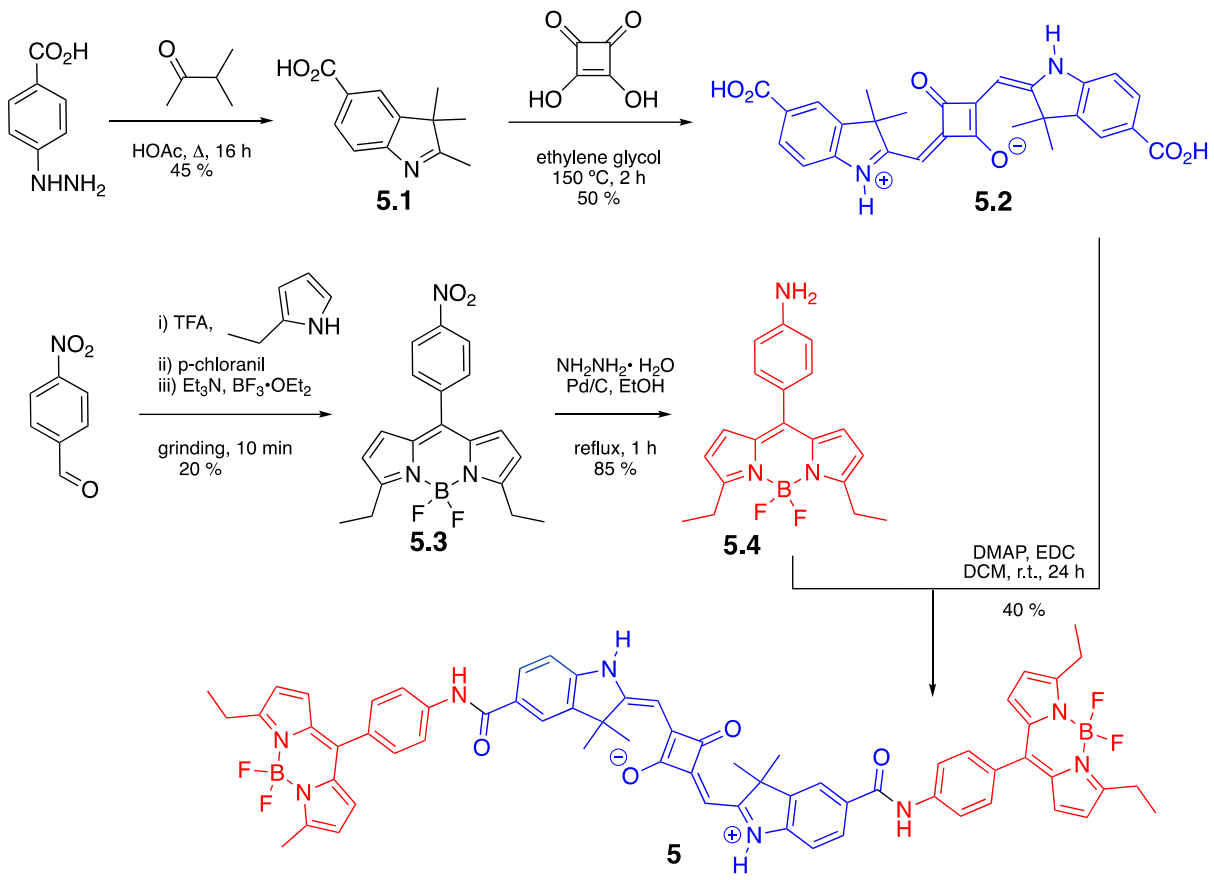

Scheme 4. Synthesis of a novel BODIPY-SQ-BODIPY viscometer **5**.

With dyes **5.2** and **5.4** in hand, synthesis of **5** was attempted (Scheme 4). To our surprise the reaction appeared quite inefficient, leading to a number of products, with the desired dye **5** being the minor product. Fortunately, it was found that increasing the amount of the base (i.e., DMAP) led to reproducible formation of the product, albeit in moderate yields.

Although further optimization of the reaction conditions is required to make the synthesis of **5** practical and useful, the material obtained during these exploratory studies prompted the spectroscopic investigation of the capabilities of **5** to act as molecular viscometer. Towards this end, steady-state fluorescence emission measurements of **5** were conducted in methanol and

glycerol (Figure 12). Methanol, used as a medium of low viscosity, should favor free rotation of the BODPY unit around the squarine core, resulting in a fully conjugated planar conformation (Figure 12) which should favor efficient resonance transfer from BODIPY to squaraine. On the other hand, in a medium of high viscosity, i.e., glycerol, the rotation should be hindered, resulting in a twisted (i.e., non-planar) conformation of **5**, which should inhibit the transfer from BODIPY to squaraine. The results depicted in Figure 12 unambiguously confirmed the ability of **5** to act as a molecular viscometer.

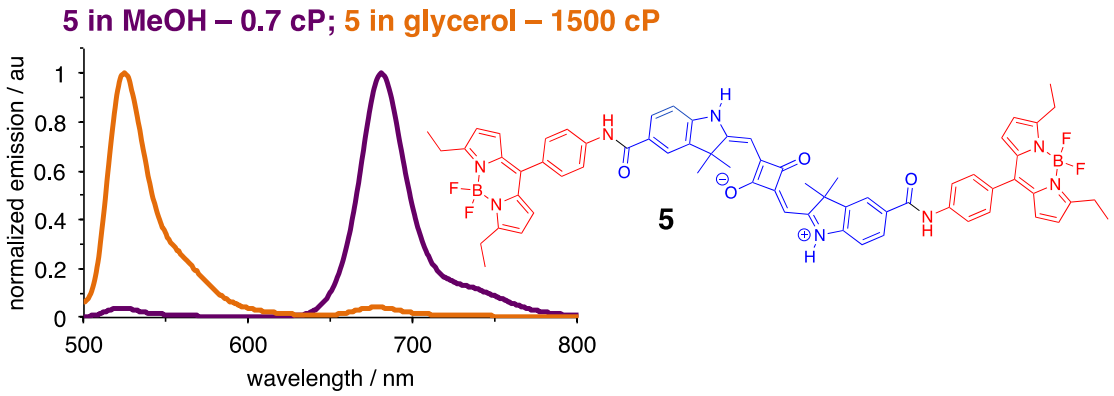

Figure 12. Steady-state fluorescence emission spectra of **5** in media of various viscosity. Conditions: λex = 480 nm; [**5**] = 2 μM. Viscosity: MeOH = 0.7 cP; glycerol = 1500 cP.

CONCLUSIONS

Molecular viscometers that operate in a ratiometric regime are viable tools for studying micro-viscosity in many chemical and biological systems. For these viscometers to be practically useful, synthetic approaches must be operationally simple, facile, efficient, and modular. Previously developed molecular viscometer **1** fulfilled some of the requirements, yet the final synthetic step leading to molecular viscometer **1** (Scheme 1) proved to be completely inefficient. As an alternative, the conceptually similar but synthetically more accessible molecular viscometer **5** (Scheme 5) was synthesized. As a viscometer, **5** exhibited the same ratiometric characteristics in response to changes of the viscosity of the media as **1**. Future studies will focus on further optimization of the synthesis of **5** as well as on the synthesis of other BODIPY-squaraine-based viscometers that are similar to **5**, in order to establish a structure-property relationship that will allow for designing versatile ratiometric viscometers with desired characteristics.

ACKNOWLEDGEMENTS

I would like to thank Phobe Pham for the synthesis of several compounds required for the synthesis of aza-BODIPY dyes **1.1** and **3.1** as well as Jeanne Favret for providing compound **5.1**. I would like to acknowledge the Professor D.E. Minter Endowment Fund for Undergraduate Research and the Dean's Research Initiative Grant for financial support.

MATERIALS AND METHODS

All reagents and solvents were purchased from the commercial sources (Sigma-Aldrich, Acros, and TCI) and were used as received. NMR spectra were acquired on a Bruker Ascend 400 (400 MHz) spectrophotometer The chemical shifts are reported in ppm (δ) from the residual solvent peak (DMSO: 2.51 ppm) or TMS (0.00 ppm). Chemical shifts of ^{19}F and ^{11}B resonances are not referenced. Multiplicities are reported as: s – singlet, bs – broad singlet, d – doublet, dd – doublet of doublets, ddd – doublet of doublet of doublets, t – triplet, q – quartet, p – pentet, sext – sextet, m – multiplet.

Absorbance and fluorescence emission measurements are performed using Agilent Gary 60 and Shimadzu RF-5301PC, respectively, with 1 cm quartz cells and resolution of 1 nm. Fluorescence measurements were carried out as follows: excitation and emission slits were 5 nm and 5 nm, sensitivity low.

Reactions were monitored by TLC (silica gel 60 F254) and the spots were visualized by UV or I2. Column chromatography was performed using silica gel (SiliaFlash P60, 40-63 μm/230-400 mesh; SILICYCLE) as the stationary phase. Armor beads (Chemglass) bath was used for all thermal reactions.

SYNTHESIS OF DYES AND PRECURSORS

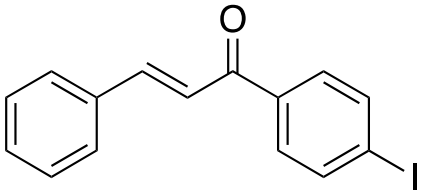

Synthesis of 1.2: A round bottom flask was charged with stirring bar, NaOH (0.5 g, 12.18 mmol) and MeOH (20 ml), and the mixture was stirred at room temperature for 30 min. Next, benzaldehyde (0.82 ml, 8.12 mmol) and 4-iodobenzophenone (2.0 g, 8.12 mmol) were added, and the mixture was vigorously stirred for 2 h at room temperature. The reaction mixture was filtered, and the solid washed with MeOH (30 ml). The filtrate was roto vaped, and the residue was recrystallized from MeOH. Both solid fractions were combined to give **1.2** (2.4 g, 90 % yield) as an off-while/beige solid.

^{1}H NMR (400 MHz, $CDCl_3$) δ 7.87 (d, *J* = 8.4 Hz, 2H), 7.82 (d, *J* = 15.6 Hz, 1H), 7.7.3 (d, *J* = 8.4 Hz, 1H), 7.64 (m, 2H), 7.47 (d, *J* = 15.6 Hz, 1H), 7.43 (m, 3H).

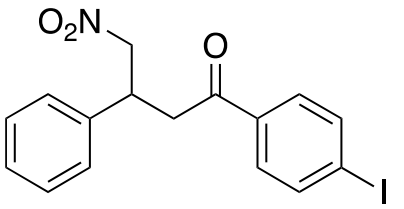

Synthesis of 1.3: Round bottom flask was charged with stirring bar, compound **1.2** (4.0 g, 12.0 mmol), iPr2NH (8.0 ml, 56.9 mmol), and CH3NO2 (3.3 ml, 60.1 mmol). The flask was fitted with reflux condenser and placed in 60 ºC beads bath under stirring for 24 h. Next, the reaction mixture was diluted with ethyl acetate (100 ml), washed with H2O (100 ml x 20, 1m HCl (200 ml x 2), brine (100 ml). Volatiles were removed in vacuo, and the residue was recrystallized (EtOH) to give **1.3** (2.2 g, 47 % yield) as a white solid.

1H NMR (400 MHz, CDCl3) δ 7.82 (d, J = 8.4 Hz, 2H), 7.61 (d, J = 8.4 Hz, 2H), 7.33 (m, 2H), 7.27 (m, 3H), 4.81 (dd, J = 12.4, 6.8 Hz, 1H), 4.68 (dd, J = 12.8, 7.8 Hz, 1H), 4.20 (pent, J = 7.2 Hz, 1H), 3.41 (dd, J = 7.2, 3.6 Hz, 2H).

Synthesis of 1.1: Round bottom flask was charged with stirring bar, compound **1.3** (1.5 g, 3. 8 mmol), NH_4OAc (20 g, 411.2 mmol), and CF_3CH_2OH (20 ml). The flask was fitted with reflux condenser and placed in 100 ºC beads bath under stirring for 24 h. The reaction was cooled to room temperature, filtered, washed with EtOH (300 ml), dried in vacuum to give **1.4** (700 mg, 52 % yield) as a purple-blue solid, which was used for the next step without further purification.

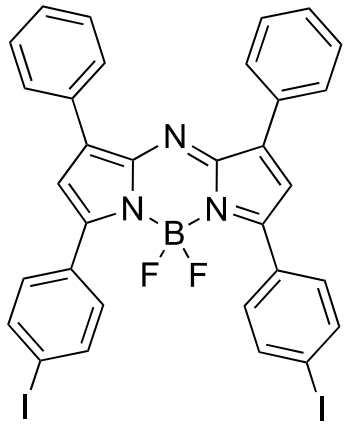

1.4 (640 mg, 0.91 mmol) was placed into a round bottom flask equipped with a stirring bar, followed by addition of $Cl(CH_2)_2Cl$ (10 ml), Et_3N (10 ml, 71.7 mmol), and BF_3•Et_2O (10 ml, 81 mmol; added slowly via syringe under stirring). The flask was fitted with a reflux condenser and placed into 100 ºC armor beads bath for 6 h under vigorous stirring. The reaction mixture was cooled to room temperature, diluted with CH_2Cl_2 (100 ml) and washed with 1 M HCl (100ml), brine (100 ml). The volatiles were removed in vacuo, and the residue was purified via column chromatography (SiO_2, $CHCl_3$) to give **1.1** (562 mg, 75 % yield) as a bronze solid.

^{1}H NMR (400 MHz, $CDCl_3$) δ 8.04 (m, 4H), 7.85 (d, J = 8.8 Hz, 4H), 7.77 (d, J = 8.4 Hz, 2H), 7.46 (m, 4H), 7.02 (s, 2H).

^{19}F NMR (376 MHz, $CDCl_3$): δ – 131.10 (q, J = 30 Hz).

^{11}B NMR (128 MHz, $CDCl_3$): δ 0.85 (t, J = 31 Hz).

Synthesis of 3.2: A round bottom flask was charged with stirring bar, NaOH (1.0 g, 24.4 mmol) and MeOH (30 ml), and the mixture was stirred at room temperature for 30 min. Next,

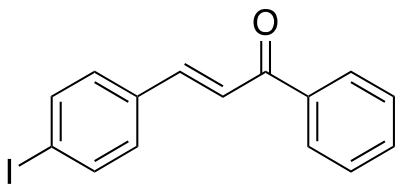

4-iodobenzaldehyde (3.03 g, 12.98 mmol) and acetophenone (1.5 ml, 12.98 mmol) were added, and the mixture was vigorously stirred for 3 h at room temperature. The reaction mixture was filtered, and the solid washed with MeOH (30 ml), H_2O (15 ml), then MeOH (30 ml). The filtrate was rotovaped, and the residue was recrystallized from MeOH. Both solid fractions were combined to give 3.2 (4.26 g, 83 % yield) as off-while/beige solid.

^{1}H NMR (400 MHz, $CDCl_3$) δ 8.01 (d, J = 7.2 Hz, 2H), 7.76 (d, J = 8.4 Hz, 2H), 7.73 (d, J = 16.0 Hz, 1H), 7.60 (d, J = 7.4 Hz, 1H), 7.53 (d, J = 16.0 Hz, 1H), 7.51 (t, J = 7.6 Hz, 2H), 7.37 (d, J = 8.4 Hz, 1H).

Synthesis of 3.3: Round bottom flask was charged with stirring bar, compound **3.2** (3.9 g, 11.7 mmol), iPr_2NH (8.0 ml, 56.9 mmol), and CH_3NO_2 (3.3 ml, 60.1 mmol). The flask was fitted

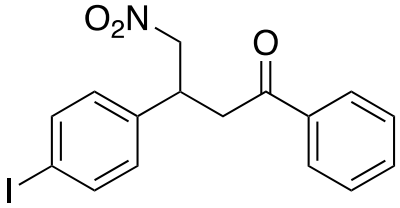

with reflux condenser and placed in 60 ºC beads bath under stirring for 6 h. Next, the reaction mixture was diluted with ethyl acetate (100 ml), washed with H_2O (100 ml x 20, 1m HCl (200 ml x 2), brine (100 ml). Volatiles were removed in vacuo, and the residue was recrystallized (EtOH) to give **3.3** (3.4 g, 75 % yield) as a white solid.

^{1}H NMR (400 MHz, $CDCl_3$) δ 7.91 (m, 2H), 7.66 (d, J = 8.4 Hz, 2H), 7.59 (t, J = 7.6 Hz, 1H), 7.46 (d, J = 8.0 Hz, 2H), 7.05 (d, J = 8.4 Hz, 2H), 4.81 (dd, J = 12.4, 6.4 Hz, 1H), 4.65 (dd, J = 14.8, 8.2 Hz, 1H 4.19 (pent, J = 7.2 Hz, 1H), 3.43 (dd, J = 7.2, 3.8 Hz, 2H).

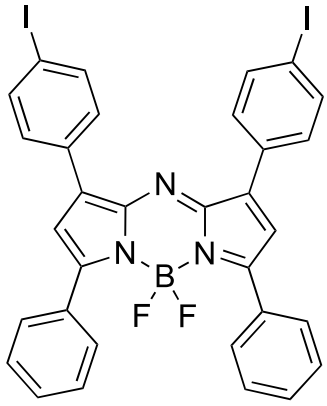

Synthesis of 3.4: Round bottom flask was charged with stirring bar, compound 3.3 (6.0 g, 15.2 mmol), NH_4OAc (76 g, 1.39 mol), and CF_3CH_2OH (80 ml). The flask was fitted with reflux condenser and placed in 100 ºC beads bath under stirring for 24 h. The reaction was cooled to room temperature, filtered, and the black-purple solid was washed with EtOH (450 ml), dried in vacuum to give **3.4** (2.1 g, 40 % yield) as black-purple solid, which was used for the next step without further purification.

3.4 (320 mg, 0.45 mmol) was placed into a round bottom flask equipped with a stirring bar, followed by addition of $Cl(CH_2)_2Cl$ (10 ml), Et_3N (5 ml, 35.9 mmol), and $BF_3•Et_2O$ (5 ml, 40.5 mmol; added slowly via syringe under stirring). The flask was fitted with a reflux condenser and placed into 100 ºC armor beads bath for 6 h under vigorous stirring. The reaction mixture was cooled to room temperature, diluted with CH_2Cl_2 (100 ml) and washed with 1 M HCl (100ml), brine (100 ml). The volatiles were removed in vacuo, and the residue was washed with acetone (150 ml) to give **3.4** (143 mg, 85 % yield) as a bronze solid.

^{1}H NMR (400 MHz, $CDCl_3$) δ 8.02 (m, 4H), 7.78 (m, 8H), 7.48 (m, 4H), 7.02 (s, 2H).

^{19}F NMR (376 MHz, $CDCl_3$): δ – 131.35 (q, J = 30 Hz).

^{11}B NMR (128 MHz, $CDCl_3$): δ 0.85 (t, J = 31 Hz).

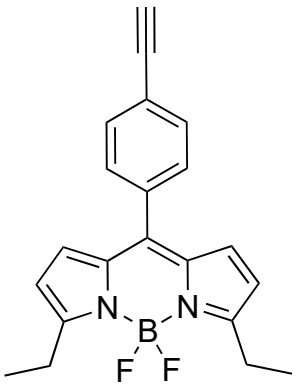

Synthesis of 4: In the hood, 2-ethylpyrrole (2.0 ml, 19.5 mmol), 4-ethynylbenzaldehyde (1.2 g, 9.2 mmol) were mixed in a mortar with the pestle till the formation of homogenous mixture was observed. Trifluoroacetic acid (3-4 drops) was added drop-wise to the mixture under grinding to form a sticky brown paste, followed by addition of CH_2Cl_2 (3 ml), and mixing/grinding with the pestle to form homogeneous brown-yellow mixture. Next, p-chloranil (3.2 g, 12.6 mmol) was added in one portion, and the red mixture was grinded for 3 minutes. Subsequently, Et_3N (15 ml, 107.6 mmol) was added, and grinded for 3 minutes to obtain green-brown-yellow paste. Next, behind the protecting glass shield, BF_3•Et2O (15 ml, 121.5 mmol) was slowly added next via syringe while grinding. The red fuming mixture was grinded for another 3 minutes. The fluid paste was transferred into the separatory funnel with CH_2Cl_2 (400 ml) and washed with 1 M HCl (400 ml x 2), and brine (400 ml). Volatiles were removed in vacuo, and the residue was subjected to column chromatography (SiO_2/$CHCl_3$) to give **4.2** (0.48 g, 15 % yield) as a red solid.

^{1}H NMR (400 MHz, $CDCl_3$) δ 7.60 (d, J = 8.4 Hz, 4H), 7.46 (d, J = 8.4 Hz, 2H), 6.71 (d, J = 4.4 Hz, 2H), 6.35 (d, J = 4.4 Hz, 2H). 3.21 (s, 1H), 3.08 (q, J = 7.6 Hz, 4H), 1.34 (t, J = 7.6 Hz, 6H).

^{19}F NMR (376 MHz, $CDCl_3$): δ – 145.27 (q, J = 33 Hz).

^{11}B NMR (128 MHz, $CDCl_3$): δ 0.96 (t, J = 33 Hz).

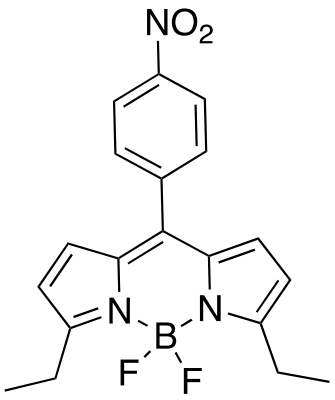

Synthesis of 5.3: In the hood, 2-ethylpyrrole (1.0 ml, 9.8 mmol), 4-nitrobenzaldehyde (0.75 g, 4.8 mmol) were mixed in a mortar with the pestle till the formation of homogenous mixture was observed. Trifluoroacetic acid (3-4 drops) was added drop-wise to the mixture under grinding to form a sticky brown paste, followed by addition of CH_2Cl_2 (3 ml), and mixing/grinding with the pestle to form homogeneous brown-yellow mixture. Next, p-chloranil (1.9 g, 7.5 mmol) was added in one portion, and the red mixture was grinded for 3 minutes. Subsequently, Et_3N (6.0 ml, 43.0 mmol) was added, and grinded for 3 minutes to obtain green-brown-yellow paste. Next, behind the protecting glass shield, BF_3•Et_2O (6.0 ml, 48.9 mmol) was slowly added next via syringe while grinding. The red fuming mixture was grinded for another 3 minutes. The fluid paste was transferred into the separatory funnel with CH_2Cl_2 (200 ml) and washed with 1 M HCl (200 ml x 2), and brine (200 ml). Volatiles were removed in vacuo, and the residue was subjected to column chromatography (SiO_2/$CHCl_3$) to give nitro-precursor for **5.3** (0.35 g, 20 % yield) as a red solid.

^{1}H NMR (400 MHz, $CDCl_3$) δ 8.35 (d, J = 8.4 Hz, 2H), 7.68 (d, J = 8.4 Hz, 2H), 6.64 (d, J = 4.0 Hz, 2H), 6.38 (d, J = 4.0 Hz, 2H), 3.09 (q, J = 7.2 Hz, 4H), 1.35 (t, J = 7.2 Hz, 6H).

^{19}F NMR (376 MHz, $CDCl_3$): δ – 145.13 (q, J = 33 Hz).

^{11}B NMR (128 MHz, $CDCl_3$): δ 0.94 (t, J = 32 Hz).

Synthesis of 5.4: A pressure tube was charged with a stirring bar, **5.3** (190 mg, 0.51 mmol), Pd/C (100 mg), and EtOH (4.0 ml), followed by $NH_2NH_2•H_2O$ (0.1 ml). The tube was capped and placed into 100 ºC armor beads bath under stirring for 1 h. Next, the pressure tube was cooled to room temperature, and Na_2SO_4 (0.5 g) was added, and the mixture was stirred for 5 min, filtered, and the solids washed with CH_2Cl_2 (100 ml). The volatiles were removed in vacuo, and the residue was dissolved in CHCl3 (5 ml), and passed through a short pad of SiO_2, washed with $CHCl_3$. All liquid fractions were combined, roto vaped to give 5.4 (0.15 g, 85 % yield) as a red solid.

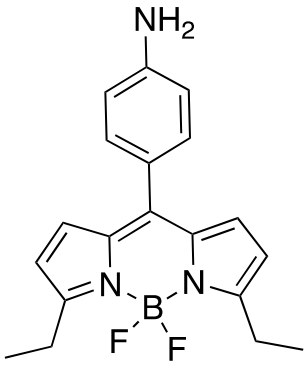

^{1}H NMR (400 MHz, $CDCl_3$) δ 7.31 (d, J = 8.5 Hz, 2H), 6.81 (d, J = 4.2 Hz, 2H), 6.71 (d, J = 8.5 Hz, 2H), 6.33 (d, J = 4.2 Hz, 2H), 3.07 (q, J = 7.6 Hz, 4H), 1.33 (t, J = 7.6 Hz, 6H).

^{19}F NMR (376 MHz, $CDCl_3$): δ – 145.06 (q, J = 33 Hz).

^{11}B NMR (128 MHz, $CDCl_3$): δ 1.02 (t, J = 33 Hz).

Synthesis of 5.2: A round bottom flask equipped with a magnetic stirring bar was charged with compound **5.1** (325 mg, 1.68 mmol), squaric acid (92 mg, 0.8 mmol), and polyethylene glycol/PEG400 (8 ml). The flask was fitted with a condenser and placed in 150 ºC armor beads bath for 2 h. Next, the flask was cooled to room temperature, and the content poured into brine (100 ml). The resulting solid was filtered, washed with water (200 ml), and then

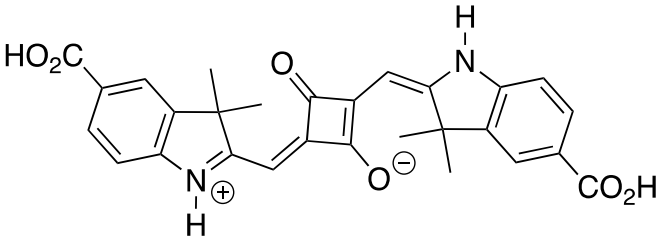

washed with acetone (100 ml), and died under vacuum to give 5.2 (407 mg, 50 % yield) as a green solid.

^{1}H NMR (400 MHz, DMSO-d_6) δ 12.87 (m 4H), 8.03 (d, J = 1.2 Hz, 2H), 7.93 (dd, J = 8.0, 1.6 Hz, 2H), 7.33 (d, J = 8.0 Hz, 2H), 5, 72 (s, 2H), 1.49 (s, 12H).

Synthesis of 5: A screw-cap via was charged with stirring bar, 5.2 (28 mg, 0.06 mmol), 5.4 (45 mg, 0.13 mmol), DMAP (34 mg, 0.28 mmol), EDC (34 mg, 0.18 mmol), and CH_2Cl_2 (2 ml). The vial was tightly capped and vigorously stirred at room temperature for 24 h. Next, the reaction mixture was directly subjected to column chromatography (SiO_2, CH_3Cl/ethyl acetate 2/1) the fractions containing the product were combined, volatiles removed in vacuo, and the solid residue was washed with acetone, and dried under vacuum to give **5** (27 mg, 40 % yield) as a bronze solid.

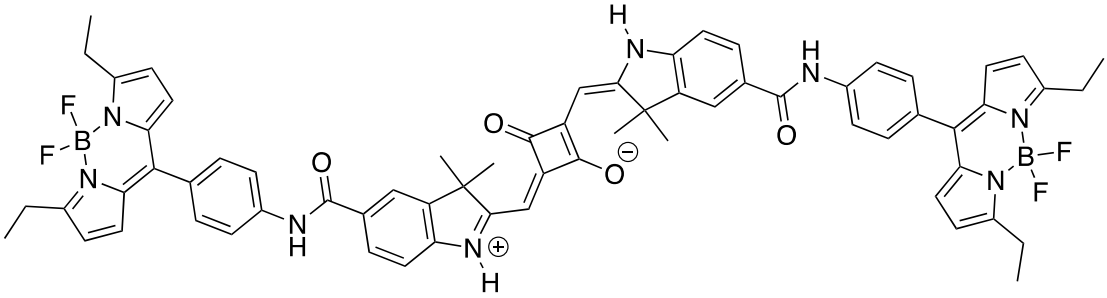

^{1}H NMR (400 MHz, DMSO-d_6) δ 12.96 (bs, 2H), 10.50 (s, 2H), 8.11 (s, 2H), 8.02 (m, 6H), 7.63 (d, J = 8.8 Hz, 4H), 7.44 (d, J = 8.0 Hz, 2H), 6.92 (d, J = 4.4 Hz, 4H), 6.58 (d, J = 4.0 Hz, 4H), 5.75 (s, 2H), 2.96 (q, J = 7.6 Hz, 4H), 1.55 (s, 12H), 1.29 (t, J = 7.6 Hz, 12H).

^{19}F NMR (376 MHz, DMSO-d_6): δ – 142.60 (q, J = 32 Hz).

^{11}B NMR (128 MHz, DMSO-d_6): δ 0.83 (t, J = 33 Hz).

REFERENCES

1. Ma, C., Sun, W., Xu, L., Qian, Y., Dai, J., Zhong, G., Hou, Y., Liu, J., & Shen, B. (2020). A minireview of viscosity-sensitive fluorescent probes: design and biological applications. *Journal of Materials Chemistry B*, *8*(42), 9642-9651. https://doi.org/10.1039/D0TB01146K
2. Kimball, J. D., Raut, S., Jameson, L. P., Smith, N. W., Gryczynski, Z., & Dzyuba, S. V. (2015). BODIPY–BODIPY dyad: assessing the potential as a viscometer for molecular and ionic liquids. *RSC Advances*, *5*(25), 19508-19511. https://doi.org/10.1039/C4RA09757B
3. Fan, J., Hu, M., Zhan, P., & Peng, X. (2013). Energy transfer cassettes based on organic fluorophores: construction and applications in ratiometric sensing [10.1039/C2CS35273G]. *Chemical Society Reviews*, *42*(1), 29-43. https://doi.org/10.1039/C2CS35273G
4. Paez-Perez, M., & Kuimova, M. K. (2024). Molecular Rotors: Fluorescent Sensors for Microviscosity and Conformation of Biomolecules. *Angewandte Chemie International Edition*, *63*(6), e202311233. https://doi.org/https://doi.org/10.1002/anie.202311233
5. Kuimova, M. (2012). Mapping viscosity in cells using molecular rotors. *Physical chemistry chemical physics : PCCP*, *14*, 12671-12686. https://doi.org/10.1039/c2cp41674c
6. Gui, R., Jin, H., Bu, X., Fu, Y., Wang, Z., & Liu, Q. (2019). Recent advances in dual-emission ratiometric fluorescence probes for chemo/biosensing and bioimaging of biomarkers. *Coordination Chemistry Reviews*, *383*, 82-103. https://doi.org/https://doi.org/10.1016/j.ccr.2019.01.004
8. Liu, P., Mu, X., Zhang, X.-D., & Ming, D. (2020). The Near-Infrared-II Fluorophores and Advanced Microscopy Technologies Development and Application in Bioimaging. *Bioconjugate Chemistry*, *31*(2), 260-275. https://doi.org/10.1021/acs.bioconjchem.9b00610
7. Das, S., Dey, S., Patra, S., Bera, A., Ghosh, T., Prasad, B., Sayala, K. D., Maji, K., Bedi, A., & Debnath, S. (2023). BODIPY-Based Molecules for Biomedical Applications. *Biomolecules*, *13*(12). https://doi.org/10.3390/biom13121723
8. Liu, P., Mu, X., Zhang, X.-D., & Ming, D. (2020). The Near-Infrared-II Fluorophores and Advanced Microscopy Technologies Development and Application in Bioimaging. *Bioconjugate Chemistry*, *31*(2), 260-275. https://doi.org/10.1021/acs.bioconjchem.9b00610
9. Requena, S., Ponomarchuk, O., Castillo, M., Rebik, J., Brochiero, E., Borejdo, J., Gryczynski, I., Dzyuba, S. V., Gryczynski, Z., Grygorczyk, R., & Fudala, R. (2017). Imaging viscosity of intragranular mucin matrix in cystic fibrosis cells. *Scientific Reports*, *7*(1), 16761. https://doi.org/10.1038/s41598-017-17037-2
10. Teunissen, A. J. P., Pérez-Medina, C., Meijerink, A., & Mulder, W. J. M. (2018). Investigating supramolecular systems using Förster resonance energy transfer. *Chemical Society Reviews*, *47*(18), 7027-7044. https://doi.org/10.1039/c8cs00278a

11. Douady, Castilla, Rebek, Dzyuba (2013-2015). unpublished results.

12. S. L. Raut, J. D. Kimball, R. Fudala, I. Bora, R. Chib, H. Jaafari, M. K. Castillo, N. W. Smith, I. Gryczynski, S. V. Dzyuba, Z. Gryczynski, A triazine-based BODIPY trimer as a molecular viscometer. Phys. Chem. Chem. Phys. 2016, 18, 4535–4540

13.R. Chinchilla, C. Najera, Recent advances in Sonogashira reaction. Chem. Soc. Rev. 2011, 40, 5084
14. R. Chinchilla, C. Njera, The Sonogarshira reaction: a booming methodology in synthetic organic chemistry. Chem. Rev. 2007, 107, 874
15. Naseem Ahmed, Advances and emerging trends in mechanistic insights of Sonogashira-type coupling reactions towards green protocols for sustainable organic transformations. J. Organometallic Chem. 2024, 1016, 123243
16. D. D. Ta, S. V. Dzyuba, Squaraine-based optical sensors: designer toolbox for exploring ionic and molecular recognitions. Biosensors, 2021, 9, 302
17. D. D. Ta, J. M. Favret, S. V. Dzyuba, Facile synthesis of pyrrolyl-containing semisquarines in water as precursors for non-symmetric squarines. Compounds 2023, 3, 17–26
18. D. D. Ta, E. Rodriguez, S. V. Dzyuba, Glycols as novel solvents for synthesis of squaraine dyes. Tetrahedron Green Chem. 2024, 3, 100042
19. J. M. Favret, S. V. Dzyuba, unpublished results). Using developed in the lab procedure